

Constructal Design of Elliptical Conduits for Cooling of Gas Turbine Blades with External Thermal Barrier Coating

C. Bosc^{1*}, L. A. O. Rocha^{2**}, F. R. Centeno^{2***}, and F. Gutierrez^{1****}

¹UIDET–IAME, National University of La Plata (UNLP), Department of Mechanical Engineering, 1 and 47 Street, La Plata, CP 1900 Argentina

²UFRGS–Federal University of Rio Grande do Sul, Department of Mechanical Engineering, Sarmento Leite Street 425, Porto Alegre, 90050-170 Brazil

Received May 8, 2019; in final form, September 24, 2019; accepted October 17, 2019

Abstract—Gas turbines (GTs) are thermal machines used to transform the energy released in combustion with a hydrocarbon into mechanical power, in order to drive a machine or generate thrust in aircraft. The critical issue in the GT design are the parts exposed to extreme mechanical and thermal conditions, e.g., the first row of turbine blades. The GT thermal efficiency is limited by the maximum temperature the blade materials can withstand without softening or creeping. Currently, the maximum operating temperature is above the softening point of the blade material thanks to techniques of ceramic coatings of low thermal conductivity, called Thermal Barrier Coating (TBC), and techniques of blade cooling. The internal cooling of blades involves conduits inside them for air that comes from a bleed in an intermediate compressor stage. The air bleeding is around 3 to 5% of the main GT flow. This air and the heat flow that it receives are not used to generate power, so it is necessary to optimize the cooling techniques in order to control the temperature using the least amount of air and minimum heat flux evacuated, for holding the GT overall efficiency high. The present work studies the internal cooling of Elemental Gas Turbine Blade (EGTB) with a fixed thickness of the TBC and the optimization of the conduit shape and position over a cross section in 2D. The optimization is carried out by exhaustive searching method based on the Constructal Theory. The optimization of the position, size, and aspect ratio of EGTBs was done for two types of standard elliptical conduits of different geometries, uniformly distributed. Two different objective functions are analyzed: minimum maximum temperature on the metal and maximum heat evacuation efficiency. The outcome of this work establishes that the use of elliptical conduits of aspect ratio 2:5 leads to improvement in the thermal performance of cooled blades. As compared with circular conduits of the same area, elliptical conduits allow transfer of a greater amount of heat; with a correct design, they enable a lower maximum temperature on the metal. Besides, the constructal designs obtained in this study for the minimum maximum relative temperature \tilde{T}_{\max} or maximum heat evacuation efficiency ξ were not identical.

DOI: 10.1134/S1810232819040064

1. INTRODUCTION

The critical issue in a GT (Gas Turbine) design is the sections exposed to extreme conditions, such as the first fixed blades of the nozzle (vanes) and the moving blades of the first turbine. The Rotor Inlet Temperature (RIT) is the critical variable that limits the efficiency and durability of GT [1, 6].

Currently, the RIT is above the softening point of material blade, due to ceramic coatings of low thermal conductivity, known as Thermal Barrier Coating (TBC), and internal and external cooling of blades, allowing the temperature in modern turbines to exceed 1400°C [1, 7].

*E-mail: cristian.bosc@ing.unlp.edu.ar

**E-mail: luizrocha@mecanica.ufrgs.br

***E-mail: frcenteno@mecanica.ufrgs.br

****E-mail: fernando.gutierrez@ing.unlp.edu.ar

The internal cooling is carried out by means of internal conduits disposed radially in the blade body, which are to evacuate the heat coming from the hot gases in contact with the external surface. The evacuation is performed by the flow of air supplied from a compressor. This air and the heat flow that it receives are not used to generate power, so it is necessary to optimize the cooling techniques in order to control the temperature using the least amount of air and minimum heat flux evacuated, the GT overall efficiency kept high [1].

Bejan and Lorente [2] applied the Constructal Theory to study optimization of cooling conduits in gas turbines using an EGTB (Elemental Gas Turbine Blade) in reduced-scale models with circular conduits. The thermal optimization was carried out by analytical minimization of the distance travelled by the heat flow; its results are valid under the assumption that the temperature minimization is similar to minimization of the distance travelled by the heat flow L and that the optimal design divides the heat equally in multiple scale designs.

Feng et al. [4] studied the same EGTB using the Constructal Design by solving the heat diffusion with numerical methods to minimize the maximum thermal resistance. Their results establish that for a fixed ratio of the cavity area and the domain area, it is possible to optimize the conduit sizes and the domain aspect ratio and that the vertical position of one duct cannot be optimized. With respect to the simple case of one type of conduits, the configuration of multiple scales with two types of conduit sizes yields a sensible improvement in the cooling, reducing the thermal resistance by 51.3% and thus lowering the maximum temperature.

The objective of this work is to improve the internal cooling efficiency of EGTB, replacing circular multiple-scale conduits with elliptical conduits with variable aspect ratio, which gives two additional degrees of freedom in the model. Besides that, for a more representative model, a fixed thickness of the thermal barrier coating is added, and the heat transfer by convection and radiation on the boundaries is considered.

2. PHYSICAL AND MATHEMATICAL MODELS

This work focuses on the optimization design of two types of elliptical cooling conduits in an EGTB, in search for a design that minimizes the highest temperature on the metal or generates the maximum heat evacuation. The optimization is carried out by exhaustive searching methodology, the heat diffusion equation solved using the finite elements method. The analysis is performed in the steady regime in a two-dimensional blade section, as illustrated in Fig. 1a, with constant thermo-physical properties. The outer blade surface is completely wetted by a stream of combustion gases at high temperature, while the blade is internally cooled by air passing through internal elliptical conduits that run radially the blade length.

Figure 1a shows two types of elliptical conduits. Two larger conduits are fixed vertically in the blade centre; their perimeter defines *ellipse* 0. The second-type elliptical conduits are placed in the middle between two consecutive *ellipses* 0; they are called *ellipses* 1. The blade design is defined by the shape, size, and position of both conduits, causing a problem of multiple scales. Due to the vertical and horizontal symmetry of the conduit patterns, one-eighth portion of the central section of height H and base L is chosen as the numerical domain (the hatched section shown in Fig. 1b along with the imposed boundary conditions).

The numerical model is supplemented with a thermal barrier coating (TBC) of 7YSZ ceramic of 1 mm constant thickness, which is typical of land based GT [7]. The boundary conditions incorporate the heat transfer by convection and radiation at the outer edge and convection in the internal conduits through which air circulates. Due to the symmetry, the remaining surfaces are considered as adiabatic.

The outer edge is wetted by the stream of combustion gases, whose temperature is $T_\infty = 1473$ K. The external convection coefficient (h_e) is obtained from the average Nusselt number in the turbulent regime for a flat plate of a fixed length of 0.4 m [24],

$$Nu = 0.037 Re^{0.8} Pr^{1/3} = (h_e 4L) / k_\infty. \quad (1)$$

The Reynolds number is set equal to 500,000, and the thermo-physical properties of the gas stream are given by $k_\infty = 0.07868$ W/(m·K) (obtained at 1473 K) and $Pr = 0.726$ (obtained at 1473 K). Note

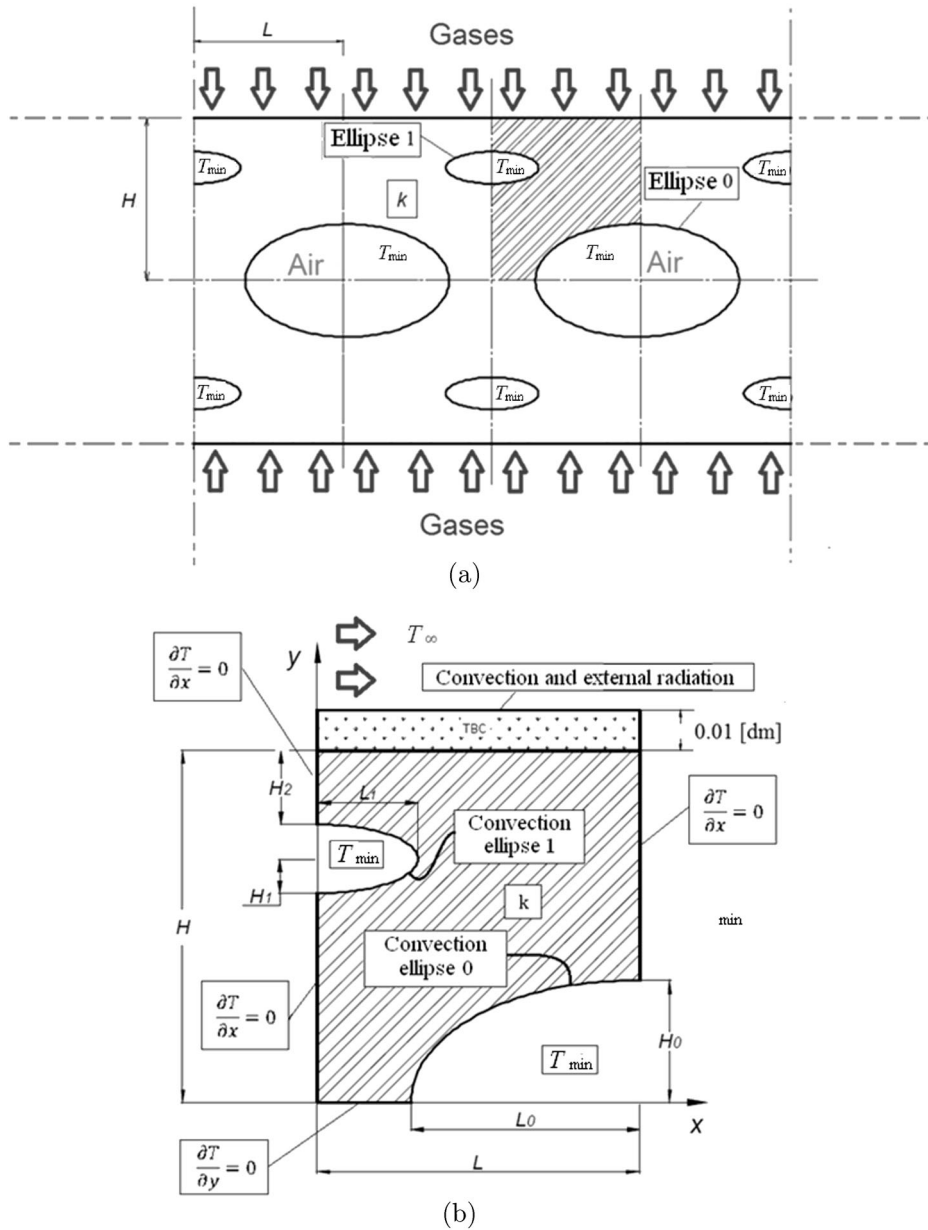


Fig. 1. (a) EGTB cross section of length $4L$ and height $2H$ with 2 types of elliptical conduits; (b) dimensions and boundary condition on the study domain; (c) EGTB with successive mesh refinement.

that at high temperature, the Prandtl number of combustion gases can be considered as the air Prandtl number.

At the conduit edges, the surface is in contact with air at the average temperature $T_{min} = 873$ K. The internal convection coefficients h_{i0} and h_{i1} for ellipses 0 and 1, respectively, are obtained from the Nusselt number for smooth pipes in the turbulent regime with an equivalent hydraulic diameter D_h [24],

$$Nu_u = 0.023 Re^{0.8} Pr^{0.4} = (h_i D_h) / k_{air}, \tag{2}$$

where the hydraulic diameters of each elliptical conduit are given by the following expressions:

$$D_{h1} = \frac{4L_1H_1}{3(L_1 + H_1) - \sqrt{(3L_1 + H_1)(L_1 + 3H_1)}},$$

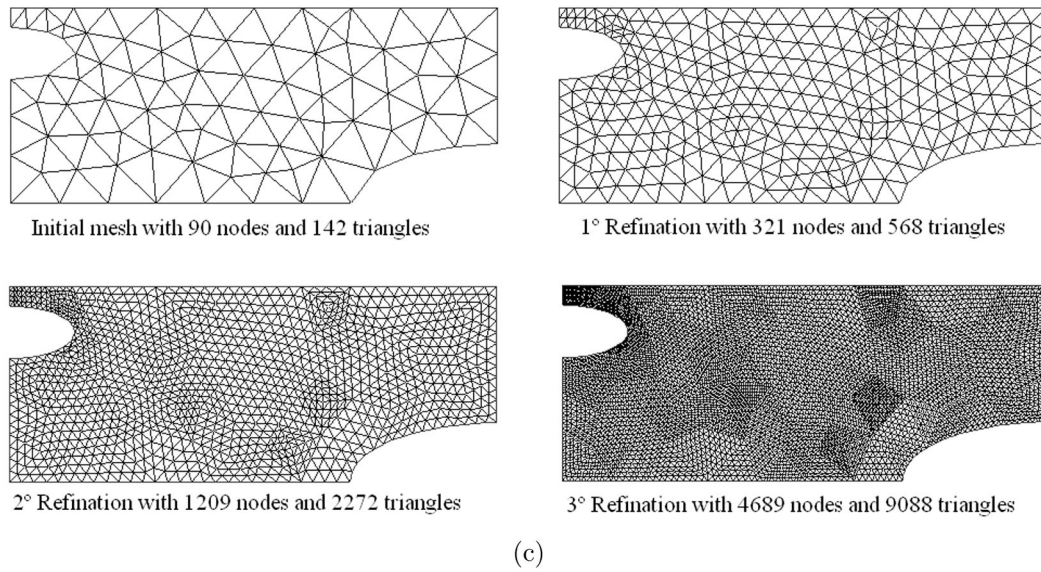


Fig. 1. (Contd.)

$$D_{h0} = \frac{4L_0H_0}{3(L_0 + H_0) - \sqrt{(3L_0 + H_0)(L_0 + 3H_0)}}, \quad (3)$$

and the Reynolds number for each conduit is obtained from its definition,

$$Re = \frac{VD_h}{\nu}. \quad (4)$$

The average velocity (V) of air circulating through the conduits is obtained from the equation that establishes the pressure drop for fully developed viscous flows circulating inside pipes in the steady regime [24]:

$$V = \left(\frac{2D_h(P_{base} - P_{tip})}{\rho f S} \right)^{1/2}, \quad (5)$$

where f is the Darcy friction factor, S is the conduit length, and ρ is the density of air. The density of air is determined from the ideal gas state equation at the average pressure and temperature of 873 K.

The Darcy friction factor for smooth tubes in the turbulent regime is determined according to the explicit first Petukhov equation [24], valid for Reynolds number between 3×10^3 and 5×10^6 .

The physical properties used to determine the internal convection coefficient are as follows:

- $k_{air} = 0.006093$ W/(m·K), air conductivity at 873 K;
- $Pr = 0.7037$, air Prandtl number at 873 K;
- $\nu = 7.806 \times 10^{-5}$ m²/s², kinematic viscosity of air at 500°C;
- $P_{tip} = 200.1$ kPa, pressure at the blade tip;
- $P_{base} = 200$ kPa, pressure at the blade base;
- $\rho = 0.7984$ kg/m³, air density at 873 K and 200.05 kPa;
- $S = 0.2$ m.

The heat transfer through the blade metallic body and the ceramic coating is entirely defined by the thermal diffusion. The metallic and ceramic parts are considered isotropic with constant thermal conductivity, k_m and k_c , respectively.

The heat diffusion is modelled by the following partial differential equation:

$$\left(\frac{\partial^2 T}{\partial x^2} + \frac{\partial^2 T}{\partial y^2} \right) = 0. \quad (6)$$

3. NUMERICAL METHODS AND SOLUTION STRATEGIES

3.1. Boundary Conditions

The heat diffusion equation, Eq. (6), is solved using the routine developed in MATLAB with the boundary conditions detailed below and shown in Fig. 1b.

With symmetry edges, the adiabatic conditions are defined as follows:

$$\frac{\partial T}{\partial x} = 0 \quad \text{for} \quad x = 0; \quad 0 \leq y \leq H - 2H_1 - H_2 \quad \text{and} \quad H - H_2 \leq y \leq H, \quad (7a)$$

$$\frac{\partial T}{\partial y} = 0 \quad \text{for} \quad y = 0; \quad 0 \leq x \leq L - L_0, \quad (7b)$$

$$\frac{\partial T}{\partial x} = 0 \quad \text{for} \quad x = L; \quad H_0 \leq y \leq H. \quad (7c)$$

The external edge at the temperature T in contact with the combustion gases at the temperature T_∞ transfers heat by convection and thermal radiation to the surroundings. The thermal-radiation heat transfer between the high temperature combustion gases at T_∞ and the ceramic coating surface at T is modelled as thermal radiation exchange between a small surface at the temperature T placed in a large cavity with the temperature T_∞ , which allows us to write the net heat exchange (over the area WL) as [24]

$$\frac{q}{WL} = k_c \frac{\partial T}{\partial y} = h_e(T_\infty - T) + \sigma\varepsilon(T_\infty^4 - T^4) \quad \text{for} \quad y = H \quad \text{and} \quad 0 \leq x \leq L. \quad (8)$$

With the conduit surfaces at the temperature T and the air inside them at the temperature T_{\min} , the heat exchange by convection is described as follows:

$$\text{Convection at ellipse 0:} \quad k_m \frac{\partial T}{\partial r} = h_{i0}(T - T_{\min}) \quad \text{for} \quad H_0 \leq r \leq L_0 \quad \text{and} \quad \pi/2 \leq \theta \leq \pi, \quad (9)$$

$$\text{Convection at ellipse 1:} \quad k_m \frac{\partial T}{\partial r} = h_{i1}(T - T_{\min}) \quad \text{for} \quad H_1 \leq r \leq L_1 \quad \text{and} \quad -\pi/2 \leq \theta \leq \pi/2. \quad (10)$$

In steady-state conditions, the net heat flux into the domain must be equal to the heat flux evacuated through the cooling conduits.

3.2. Dimensionlessness of the problem

To reduce the quantity of variables and make the optimization process feasible, the problem is made dimensionless as follows.

The relative temperature of the blades is defined as

$$\tilde{T} = \frac{T - T_{\min}}{T_\infty - T_{\min}}. \quad (11)$$

The distance perpendicular to the plane is taken equal to unity,

$$W = 1. \quad (12)$$

The lengths become dimensionless from the square root of the domain area, given as

$$A = HL, \quad (13)$$

$$(\tilde{x}, \tilde{y}, \tilde{H}, \tilde{L}, \tilde{H}_0, \tilde{L}_0, \tilde{H}_1, \tilde{L}_1, \tilde{H}_2) = \frac{(x, y, H, L, H_0, L_0, H_1, L_1, H_2)}{\sqrt{A}}. \quad (14)$$

The dimensionless form of the heat diffusion equation, Eq. (6), is as follows:

$$\left(\frac{\partial^2 \tilde{T}}{\partial \tilde{x}^2} + \frac{\partial^2 \tilde{T}}{\partial \tilde{y}^2} \right) = 0. \quad (15)$$

The heat transfer capacity over different configurations is analysed using the heat evacuation efficiency indicator, defined as

$$\xi = \frac{q/(kW)}{T_{\max} - T_{\min}}. \quad (16)$$

So, the dimensionless heat evacuation efficiency becomes

$$\xi = \frac{q/kW}{\tilde{T}_{\max} \cdot (T_{\infty} - T_{\min})}. \quad (17)$$

The configuration with the highest heat flux q and lowest maximum relative blade temperature \tilde{T}_{\max} will have the highest efficiency and therefore the highest ξ value, where the rest of the variables are constant for the model.

The corresponding dimensionless boundary conditions are as follows.

- Adiabatic surfaces:

$$\frac{\partial \tilde{T}}{\partial \tilde{x}} = 0 \quad \text{for} \quad \tilde{x} = 0; \quad 0 \leq \tilde{y} \leq \tilde{H} - 2\tilde{H}_1 - \tilde{H}_2 \quad \text{and} \quad \tilde{H} - \tilde{H}_2 \leq \tilde{y} \leq \tilde{H}, \quad (18a)$$

$$\frac{\partial \tilde{T}}{\partial \tilde{y}} = 0 \quad \text{for} \quad \tilde{y} = 0; \quad 0 \leq \tilde{x} \leq \tilde{L} - \tilde{L}_0, \quad (18b)$$

$$\frac{\partial \tilde{T}}{\partial \tilde{x}} = 0 \quad \text{for} \quad \tilde{x} = \tilde{L}; \quad \tilde{H}_0 \leq \tilde{y} \leq \tilde{H}. \quad (18c)$$

- External surface: convection + radiation

$$\frac{\partial \tilde{T}}{\partial \tilde{y}} = -\alpha_e \tilde{T}^4 - \beta_e \tilde{T}^3 - \chi_e \tilde{T}^2 - \delta_e \tilde{T} + \phi_e, \quad (19)$$

where the constants are as follows:

$$\alpha_e = \frac{\sigma \varepsilon_c \sqrt{A} (\Delta T)^3}{k_c}, \quad \beta_e = \frac{4 \sigma \varepsilon_c \sqrt{A} (\Delta T)^2 T_{\min}}{k_c}, \quad \chi_e = \frac{6 \sigma \varepsilon_c \sqrt{A} (\Delta T) T_{\min}^2}{k_c},$$

$$\delta_e = \frac{h_e \sqrt{A}}{k_c} + \frac{4 \sigma \varepsilon_c \sqrt{A} T_{\min}^3}{k_c}, \quad \text{and} \quad \phi_e = \frac{h_e \sqrt{A}}{k_c} + \frac{\sigma \varepsilon_c \sqrt{A} (T_{\infty}^4 - T_{\min}^4)}{k_c \Delta T}. \quad (20)$$

- Internal surface (conduits): convection

$$\frac{\partial \tilde{T}}{\partial \tilde{r}} = -\beta_i \tilde{T}, \quad (21)$$

where β_i is the Biot number, defined as

$$\beta_i = \frac{h_i \sqrt{A}}{k_m}. \tag{22}$$

The following thermo-physical properties are used:

$k_c = 2.5 \text{ W}/(\text{m}\cdot\text{K})$, thermal conductivity of 7YSZ ceramic at 1473 K;

$k_m = 21 \text{ W}/(\text{m}\cdot\text{K})$, thermal conductivity of Nimonic 90 at 873 K;

$\varepsilon_c = 0.6$, emissivity of 7YSZ ceramic at 1473 K;

$\sigma = 5.670373 \times 10^{-8} \text{ W}/(\text{m}^2\cdot\text{K}^4)$, Stefan–Boltzmann constant;

$T_\infty = 1473 \text{ K}$, temperature of hot gases;

$T_{min} = 873 \text{ K}$, average temperature of cooling air;

$\Delta T = T_\infty - T_{min} = 600 \text{ K}$, maximum temperature difference.

3.3. Treatment of Nonlinearities

With the nonlinearity in Eq. (19) because of the thermal radiation exchange on the outer edge proportional to the fourth power of the relative temperature, the field of relative temperature \tilde{T} over the whole blade is solved using the iterative Gauss–Newton method.

Eq. (19) is linearized as follows:

$$\frac{\partial \tilde{T}}{\partial \tilde{y}} = -\alpha_e \tilde{T}^4 - \beta_e \tilde{T}^3 - \chi_e \tilde{T}^2 - \delta_e \tilde{T} + \phi_e = S_e, \tag{23}$$

where the source term S_e is linearized with respect to the previous iteration (explicitly) in the following way:

$$\frac{S_e - S_e^*}{\tilde{T} - \tilde{T}^*} = \frac{dS_e^*}{d\tilde{T}^*}. \tag{24}$$

S_e^* is the source term evaluated from the known relative temperature \tilde{T}^* .

So, Eq. (23) takes the following form:

$$\frac{\partial \tilde{T}}{\partial \tilde{y}} + Q_e \tilde{T} = G_e, \tag{25}$$

where Q_e and G_e are constant functions solely of the relative temperature in the previous iteration \tilde{T}^* :

$$Q_e = -4\alpha_e \tilde{T}^{*3} - 3\beta_e \tilde{T}^{*2} - 2\chi_e \tilde{T}^* - \delta_e, \tag{26}$$

$$G_e = 3\alpha_e \tilde{T}^{*4} + 2\beta_e \tilde{T}^{*3} + \chi_e \tilde{T}^{*2} + \phi_e. \tag{27}$$

The field of relative temperature can be solved by following algorithm: the relative temperature \tilde{T}^* over the outer edge is estimated, and then the coefficients of Eqs. (26) and (27), which become Eq. (25) in the linear boundary condition, are calculated. The field of relative temperature over the whole blade is solved by the finite elements method, the relative temperature over the outer edge used as the next estimation, repeated until convergence. The convergence criterion adopted with respect to the previous relative temperature iterations \tilde{T}^* for all cases is

$$1 \times 10^{-4} < \frac{\tilde{T} - \tilde{T}^*}{\tilde{T}}. \tag{28}$$

3.4. Optimization: Restrictions

The dimensionless domain becomes unitary:

$$1 = \tilde{H} \tilde{L}. \quad (29)$$

The 1/4 ellipse 0 dimensionless area is

$$\phi_0 = \frac{\pi}{4} \tilde{L}_0 \tilde{H}_0. \quad (30)$$

The 1/2 ellipse 1 dimensionless area is

$$\phi_1 = \frac{\pi}{2} \tilde{L}_1 \tilde{H}_1. \quad (31)$$

The material ratio (ϕ) is defined as the ratio of the total area of the elliptical conduits to the domain area. This relationship represents the percentage of cavity in the solid domain,

$$\phi = \phi_0 + \phi_1. \quad (32)$$

Only the values of ϕ_0 that correspond to an ellipse 0 area greater or equal to the ellipse 1 area are analysed. The total area of the elliptical conduits in the EGTB is

$$A_0 = 4\phi_0 \quad \text{and} \quad A_1 = 2\phi_1. \quad (33)$$

Besides, to fulfil the condition $A_0 \geq A_1$,

$$\phi_0 \geq 1/3 \phi. \quad (34)$$

Therefore, for conduit 0 to be always equal to or greater than conduit 1, the following minimum relationship must be fulfilled: $[\phi_0/\phi]_{\min} = 0.33$. Finally, the limit for the maximum size of conduit 0 such that it occupies 90% of the assigned material ratio is defined,

$$[\phi_0/\phi]_{\max} = 0.9. \quad (35)$$

3.5. Optimization: Degrees of Freedom

Minimization of the maximum relative temperature over the metal blade $[\tilde{T}_{\max}]_{\min}$ and maximization of the heat evacuation efficiency $[\xi]_{\max}$ are separate prime objectives of this work. Groups of quotients of dimensionless variables are defined, representing five geometric degrees of freedom to be optimized for different values of fixed material relation (restriction ϕ):

$$\left\{ [\tilde{T}_{\max}]_{\min}; [\xi]_{\max}; \phi \right\} = f \left\langle \phi_0; \tilde{H}/\tilde{L}; \tilde{H}_0/\tilde{L}_0; \tilde{H}_1/\tilde{L}_1; \tilde{H}_2 \right\rangle. \quad (36)$$

The ranges of all variables used during the optimization process are presented in Table 1.

Table 1. Variables and restriction ranges


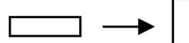
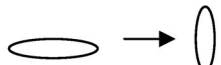
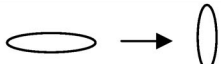
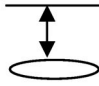
Ranges	Description
$\phi = [0.08-1.6]$	Material ratio (total conduits area /domain area)
$\phi_0 = [\phi/3-0.9\phi]$	Ellipse 0 size 
$\tilde{H}/\tilde{L} = [0.3-2]$	Domain aspect ratio 
$\tilde{H}_0/\tilde{L}_0 = [0.4-2]$	Ellipse 0 aspect ratio 
$\tilde{H}_1/\tilde{L}_1 = [0.4-2]$	Ellipse 1 aspect ratio 
$\tilde{H}_2 = [0.1 - (H - 2H_1)]$	Wall tackiness between the ellipse 1 and external surface 

Table 2. Mesh independency

Refinement	Number of triangles	\tilde{T}_{\max}^i	$ (\tilde{T}_{\max}^i - \tilde{T}_{\max}^{i-1})/\tilde{T}_{\max}^{i-1} \cdot 100$
Initial	142	0.3645	—
1°	568	0.3666	0.58
2°	2272	0.3668	0.05
3°	9088	0.3669	0.03

Table 3. Comparison of \tilde{T}_{\max} for different \tilde{H}/\tilde{L} solved with Matlab® and Comsol®

ϕ	ϕ_0	\tilde{H}/\tilde{L}	\tilde{H}_0/\tilde{L}_0	\tilde{H}_1/\tilde{L}_1	\tilde{H}_2	\tilde{T}_{\max} Matlab	\tilde{T}_{\max} Comsol	Difference [%]
0.1	0.0333	0.4	0.4	0.4	0.1	0.97586148	0.97557634	0.029%
0.1	0.0333	0.6	0.4	0.4	0.1	0.96865768	0.96836596	0.029%
0.1	0.0333	0.8	0.4	0.4	0.1	0.96435095	0.96404817	0.030%
0.1	0.0333	1	0.4	0.4	0.1	0.95975634	0.95944476	0.031%
0.1	0.0333	1.2	0.4	0.4	0.1	0.95511816	0.95479964	0.032%
0.1	0.0333	1.4	0.4	0.4	0.1	0.95057332	0.9502479	0.033%
0.1	0.0333	1.6	0.4	0.4	0.1	0.94711033	0.94687107	0.024%
0.1	0.0333	1.8	0.4	0.4	0.1	0.94660378	0.94636598	0.024%
0.1	0.0333	2	0.4	0.4	0.1	0.94610321	0.94587155	0.023%

4. GRID CONVERGENCE STUDY AND VERIFICATION

The field of dimensionless temperatures on a solid is obtained by solving Eq. (15) with the boundary conditions determined by Eqs. (18a), (18b), (18c), (21), and (25) using the finite element method (numerical routine developed in MATLAB) with a triangular grid.

For the grid convergence, the grid was continually refined until differences of less than 0.5% in two

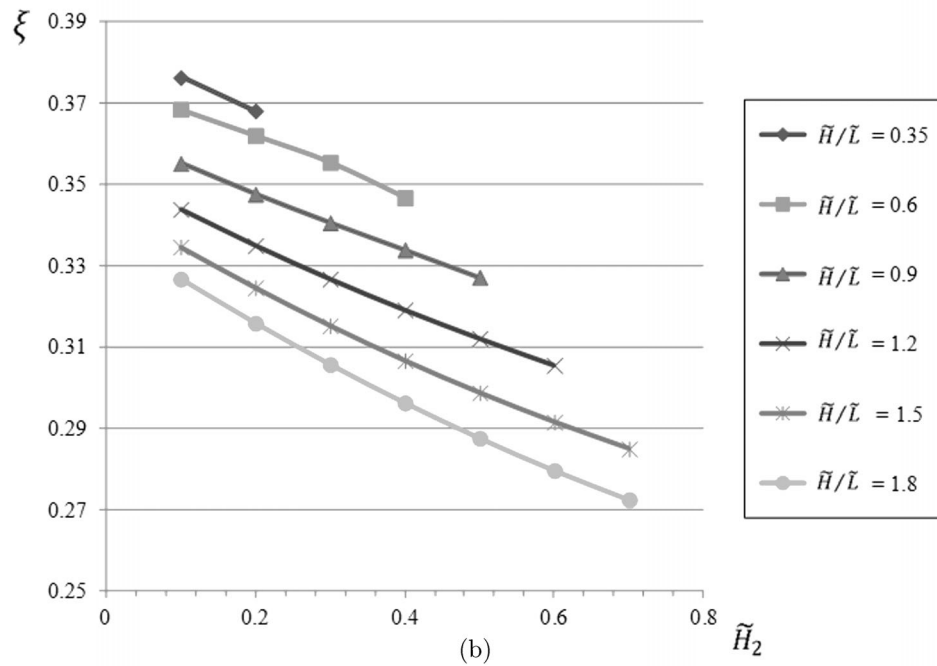
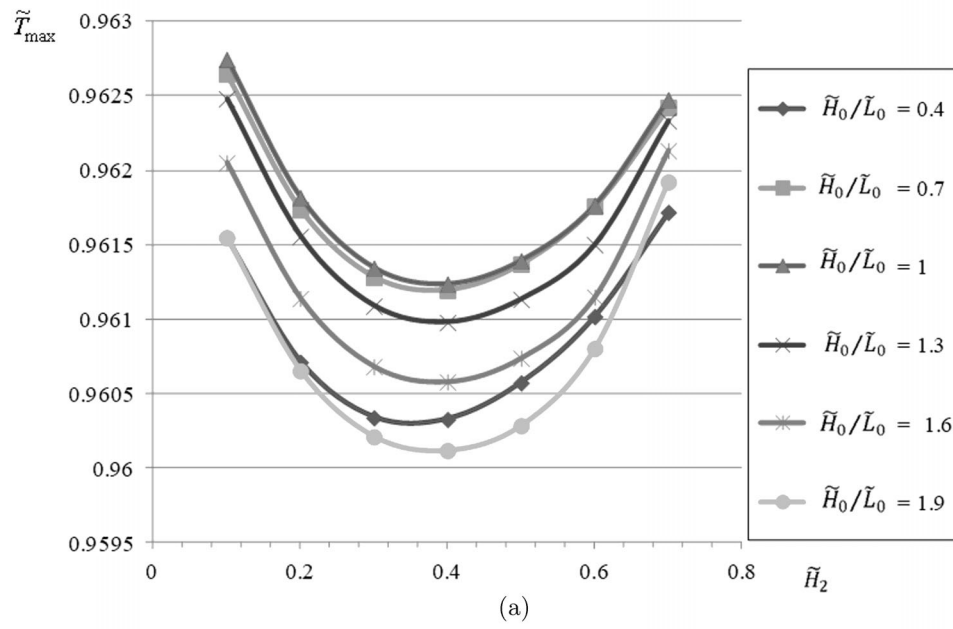


Fig. 2. (a) \tilde{T}_{\max} vs. \tilde{H}_2 for different \tilde{H}_0/\tilde{L}_0 with $\phi = 0.1$, $\phi_0 = 0.05$, $\tilde{H}/\tilde{L} = 1$, and $\tilde{H}_1/\tilde{L}_1 = 0.4$; (b) ξ vs. \tilde{H}_2 for different \tilde{H}/\tilde{L} values, with $\phi = 0.1$, $\phi_0 = 0.05$, $\tilde{H}_1/\tilde{L}_1 = 0.4$, and $\tilde{H}_0/\tilde{L}_0 = 0.4$.

successive minimum maximum relative temperatures were achieved:

$$\left| \left(\tilde{T}_{\max}^i - \tilde{T}_{\max}^{i-1} \right) / \tilde{T}_{\max}^{i-1} \right| \cdot 100 < 0.5. \tag{37}$$

Figure 1c show an example of successive refinement over an EGBT design. Table 2 presents values of \tilde{T}_{\max} obtained for each case, demonstrating that in this case the grid independency is reached in the second refinement.

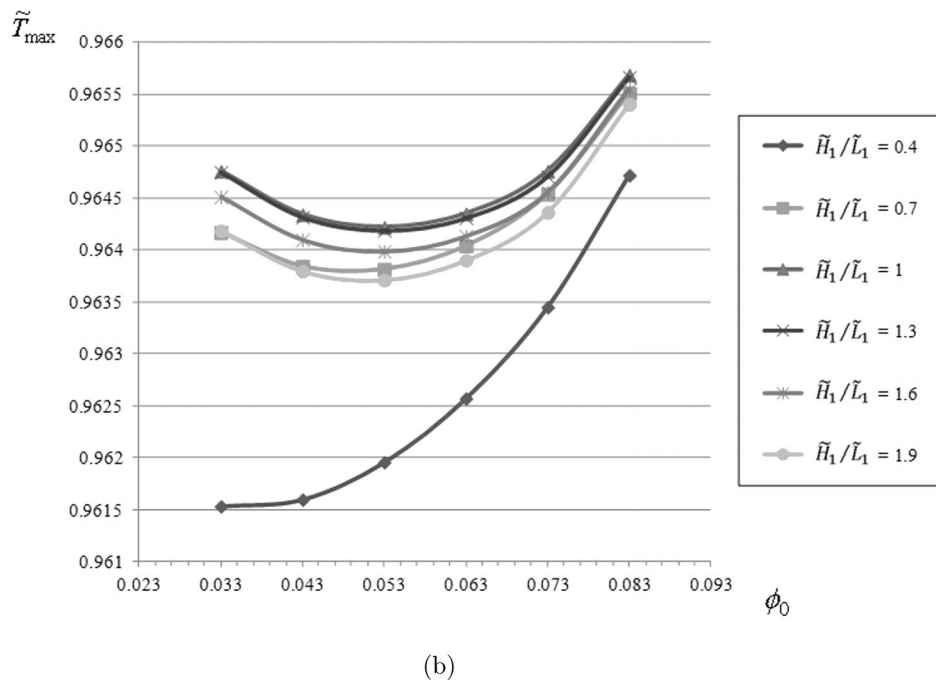
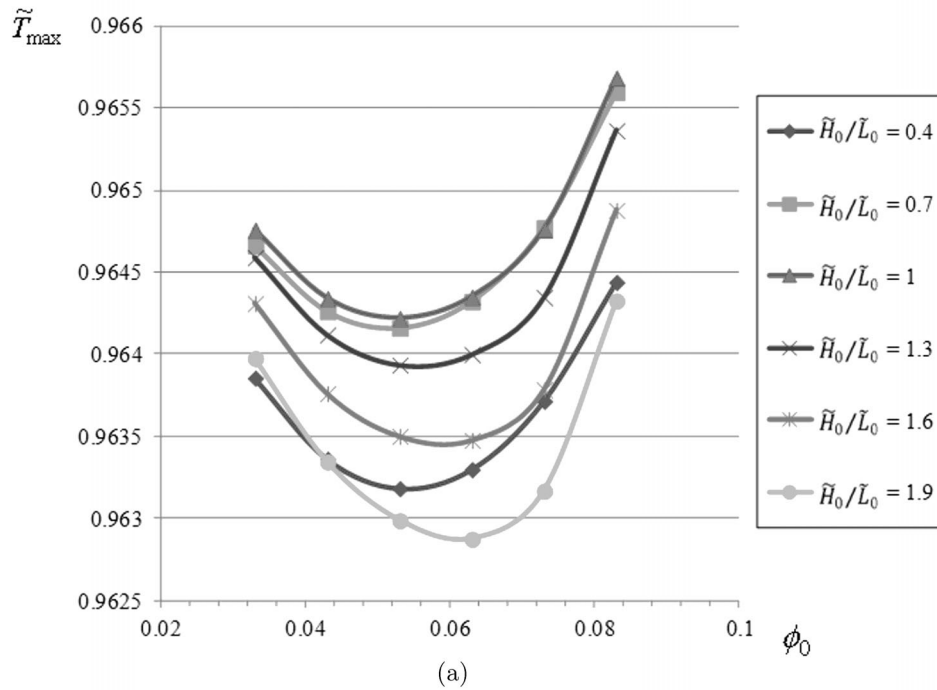
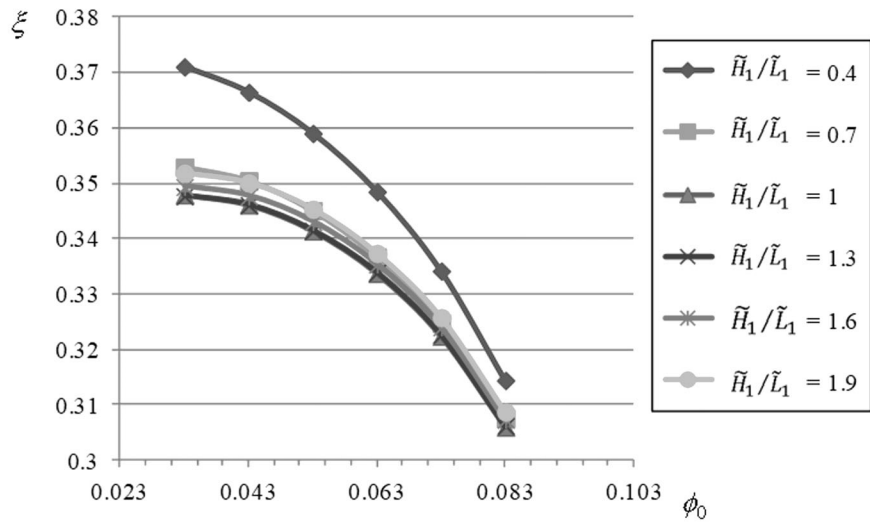
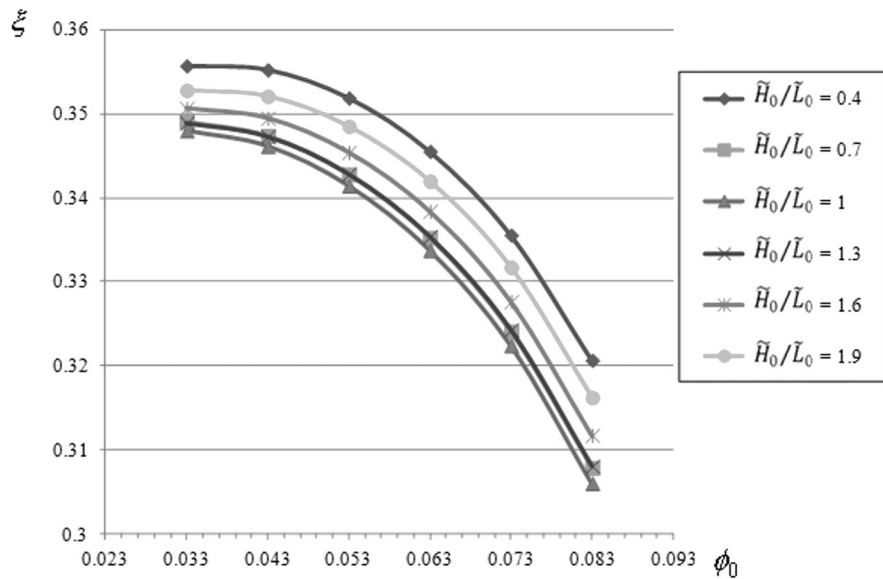


Fig. 3. \tilde{T}_{\max} vs. ϕ_0 for different (a) \tilde{H}_0/\tilde{L}_0 with $\phi = 0.1$, $\tilde{H}_1/\tilde{L}_1 = 1$, $\tilde{H}/\tilde{L} = 1$, and $\tilde{H}_2 = 0.2$; (b) \tilde{H}_1/\tilde{L}_1 with $\phi = 0.1$, $\tilde{H}_0/\tilde{L}_0 = 1$, $\tilde{H}/\tilde{L} = 1$, and $\tilde{H}_2 = 0.2$.

The numerical routine model developed in Matlab[®] (Matlab, 2016) is verified by comparison with solutions of the same problem obtained in the Comsol[®] software (Comsol, 2016). Table 3 presents an example with the maximum relative temperature \tilde{T}_{\max} for the same configuration solved by both ways, with a maximum difference of about 0.033%. So, the Matlab code can be considered as adequate to run the simulations.



(a)



(b)

Fig. 4. ξ vs. ϕ_0 for different (a) \tilde{H}_1/\tilde{L}_1 , with $\phi = 0.1$, $\tilde{H}_0/\tilde{L}_0 = 1$, $\tilde{H}_2 = 0.1$, and $\tilde{H}/\tilde{L} = 1$; (b) \tilde{H}_0/\tilde{L}_0 , with $\phi = 0.1$, $\tilde{H}_1/\tilde{L}_1 = 1$, $\tilde{H}_2 = 0.1$, and $\tilde{H}/\tilde{L} = 1$.

5. RESULTS

Figure 2a presents the results for \tilde{T}_{max} obtained for several \tilde{H}_0/\tilde{L}_0 as a function of \tilde{H}_2 , with $\phi = 0.1$, $\phi_0 = 0.05$, $\tilde{H}/\tilde{L} = 1$, and $\tilde{H}_1/\tilde{L}_1 = 0.4$, while Fig. 2b presents the results for ξ also obtained for several \tilde{H}_0/\tilde{L}_0 as a function of \tilde{H}_2 , with $\phi = 0.1$, $\tilde{H}/\tilde{L} = 1$, $\tilde{H}_0/\tilde{L}_0 = 1$, and $\tilde{H}_1/\tilde{L}_1 = 1$. For a fixed material ratio of 10% ($\phi = 0.1$), the results show that the optimum value of the wall thickness \tilde{H}_2 that generates the minimum \tilde{T}_{max} is not always found at the lower range value. So, an optimal value can be obtained at the expense of greater distance travelled by the heat, as in the case showed in Fig. 2a. The heat

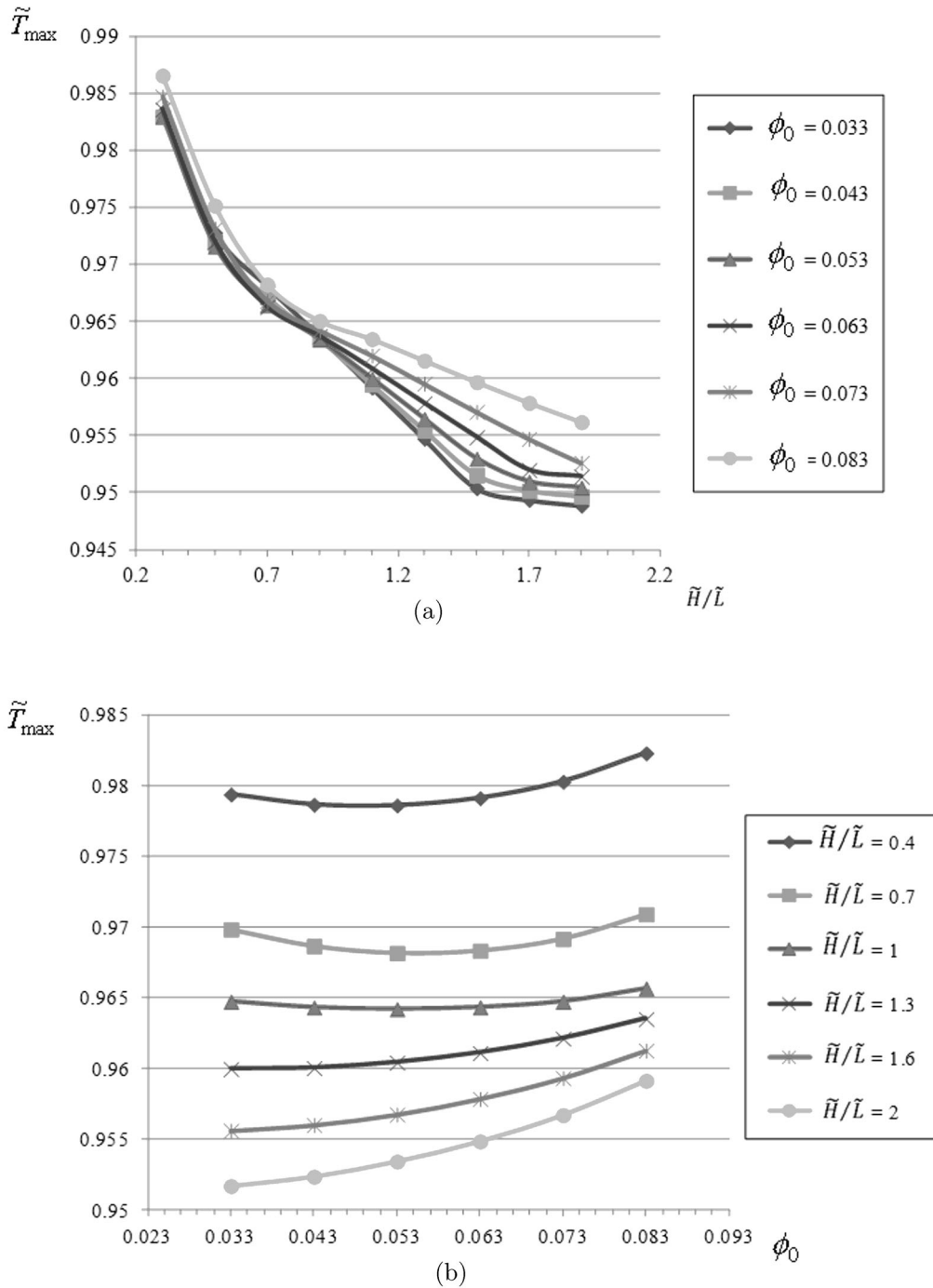


Fig. 5. (a) \tilde{T}_{\max} vs. \tilde{H}/\tilde{L} for different ϕ_0 with $\phi = 0.1$, $\tilde{H}_1/\tilde{L}_1 = 1$, $\tilde{H}_0/\tilde{L}_0 = 1$, and $\tilde{H}_2 = 0.1$; (b) \tilde{T}_{\max} vs. ϕ_0 for different \tilde{H}/\tilde{L} with $\phi = 0.1$, $\tilde{H}_1/\tilde{L}_1 = 1$, $\tilde{H}_0/\tilde{L}_0 = 1$, and $\tilde{H}_2 = 0.1$.

evacuation efficiency always increases almost linearly when the wall thickness \tilde{H}_2 decreases, for different \tilde{H}/\tilde{L} , \tilde{H}_0/\tilde{L}_0 , \tilde{H}_1/\tilde{L}_1 and ϕ_0 values, as can be seen in Fig. 2b.

In Fig. 3a, the \tilde{T}_{\max} variation is plotted against ϕ_0 for different \tilde{H}_0/\tilde{L}_0 values. One can see that for all curves there is an optimum value of ϕ_0 that generates the minimum \tilde{T}_{\max} . That means that each aspect ratio of ellipse has a unique optimal conduit size. From all curves, $\tilde{H}_0/\tilde{L}_0 = 0.4$ generates the

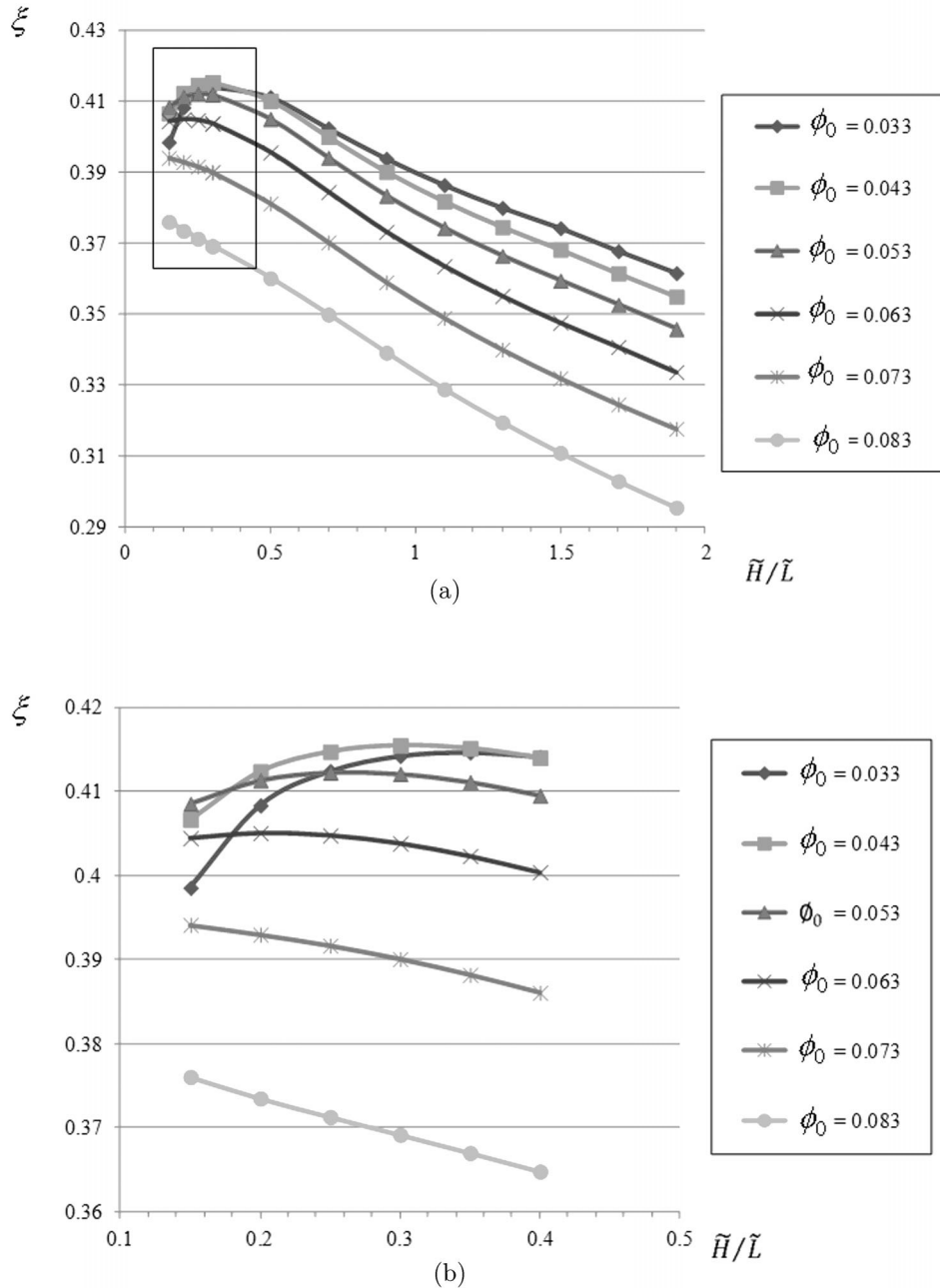


Fig. 6. (a) ξ vs. \tilde{H}/\tilde{L} for different ϕ_0 , with $\phi = 0.1$, $\tilde{H}_0/\tilde{L}_0 = 0.4$, $\tilde{H}_1/\tilde{L}_1 = 0.4$, and $\tilde{H}_2 = 0.1$; (b) Zoom over the boxed area of Fig. 6 (a).

minimum \tilde{T}_{max} for values of $\phi_0 < 0.043$, while for $\phi_0 > 0.043$ so does the curve of $\tilde{H}_0/\tilde{L}_0 = 1.9$, as can be seen in the same figure.

Figure 3b presents the \tilde{T}_{max} response as a function of ϕ_0 for constant curves \tilde{H}_1/\tilde{L}_1 . There is an optimal value for all curves, except for the case of $\tilde{H}_1/\tilde{L}_1 = 0.4$, where the \tilde{T}_{max} decreases monotonically as ϕ_0 also decreases. This thermal behaviour is explained because for $\tilde{H}_1/\tilde{L}_1 = 0.4$ it represents an ellipse 1 with a lower aspect ratio (flattened). For a fixed material ratio $\phi = 0.1$, as ϕ_0 is reduced, the ellipse 1 area becomes larger, propagating over a large part of the fixed thickness domain L. The

Minimum maximum relative temperature



Maximum heat evacuation efficiency

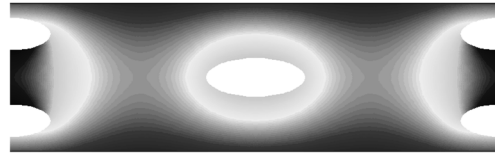


Fig. 7. Isotherms plot over optimal designs of Table 4 for minimum \tilde{T}_{\max} (left) and maximum ξ (right).

Table 4. Minimum \tilde{T}_{\max} and maximal ξ designs for $\phi = 0.1$

ϕ	ϕ_0	\tilde{H}/\tilde{L}	\tilde{H}_0/\tilde{L}_0	\tilde{H}_1/\tilde{L}_1	\tilde{H}_2	\tilde{T}_{\max}	ξ
0.1	0.043	0.3	0.4	0.4	0.1	0.983	0.42
0.1	0.033	2	0.4	0.4	0.2	0.948	0.34

minimum \tilde{T}_{\max} is reached for the minimum aspect ratio of ellipse 1 over the entire range of ϕ_0 when \tilde{H}/\tilde{L} takes values equal to or less than 1.

For different ellipse 1 aspect ratios \tilde{H}_1/\tilde{L}_1 , the heat evacuation efficiency continuously increases as ϕ_0 decreases, as well as for different ellipse 0 aspect ratios \tilde{H}_0/\tilde{L}_0 shown in Figs. 4a and 4b, respectively. Analysis of the aforementioned figures shows that the maximum efficiency is achieved for both ellipses with the lowest aspect ratio and same conduit sizes ($\phi_0 = 0.033$).

Figures 5a and 5b show the behaviour of \tilde{T}_{\max} with respect to ϕ_0 and the domain aspect ratio \tilde{H}/\tilde{L} . In Fig. 5a, it can be seen that \tilde{T}_{\max} drops as \tilde{H}/\tilde{L} increases for all values of ϕ_0 , which shows great influence of \tilde{H}/\tilde{L} on \tilde{T}_{\max} . In Fig. 5b it is shown that a domain area flattened of rectangular and square shape (represented by curves of \tilde{H}/\tilde{L} equal to 0.4, 0.7, and 1) has a unique optimal conduit area, which generate minimum \tilde{T}_{\max} with some value between the extreme range values. Meanwhile, for all curves of $\tilde{H}/\tilde{L} > 1$, ever there is a unique optimal value of $\phi_0 = 0.033$, that is, conduits of equal size (that the value of ϕ_0 represents same conduit area, see Eq. (34)). So, the optimal value of the duct size ϕ_0 is strongly dependent on the domain aspect ratio. The absolute minimum \tilde{T}_{\max} is reached with the highest aspect ratio of the domain, $\tilde{H}/\tilde{L} = 2$ and conduits of equal size. Of all the variables analysed so far, the one with the highest influence on \tilde{T}_{\max} is the domain aspect ratio and thus its correct choice can reduce \tilde{T}_{\max} by up to 3% (from 0.95 to 0.98, Fig. 5b).

The net heat flux entering the domain is a function, among other things, of the external surface temperature (which is not imposed) and the area wetted by the hot gases (of dimensionless length L and unitary depth W). Therefore, as \tilde{H}/\tilde{L} increases, the outer edge decreases, as does the net heat entering the domain. The minimum absolute value of \tilde{T}_{\max} is reached for $\phi_0 = 0.033$ and $\tilde{H}/\tilde{L} = 2$, which means the lowest transfer area and the largest ellipse 1 size (according to the established range limits) and therefore lower net heat flux introduced. The behaviour of \tilde{T}_{\max} with \tilde{H}/\tilde{L} makes impossible optimization beyond the range limits. Therefore, the optimal value of \tilde{H}/\tilde{L} for the minimum \tilde{T}_{\max} is taken as $\tilde{H}/\tilde{L} = 2$ and the remaining variables are optimized.

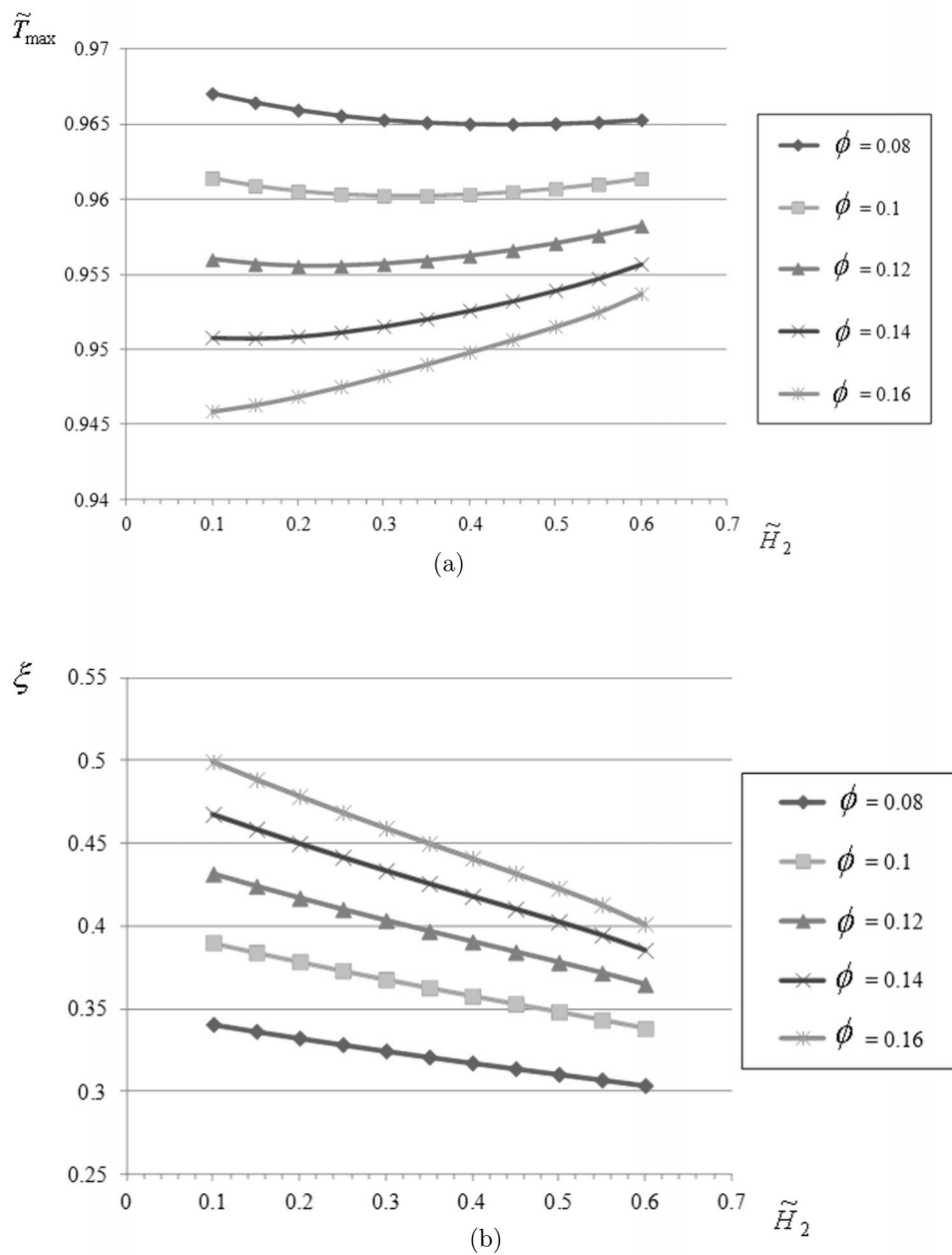


Fig. 8. (a) \tilde{T}_{\max} vs. \tilde{H}_2 for different ϕ with $\phi_0 = 0.033$, $\tilde{H}_1/\tilde{L}_1 = 0.4$, $\tilde{H}_0/\tilde{L}_0 = 0.4$, and $\tilde{H}/\tilde{L} = 1$; (b) ξ vs. \tilde{H}_2 for different ϕ with $\phi_0 = 0.033$, $\tilde{H}_1/\tilde{L}_1 = 0.4$, $\tilde{H}_0/\tilde{L}_0 = 0.4$, and $\tilde{H}/\tilde{L} = 1$.

Figure 6a presents ξ versus \tilde{H}/\tilde{L} for different ϕ_0 . The heat evacuation efficiency increases almost linearly as \tilde{H}/\tilde{L} decreases over the range [0.5–2]. The minimum efficiency is reached with the maximum domain aspect ratio, i.e., $\tilde{H}/\tilde{L} = 2$, which is a geometry that also generates the minimum \tilde{T}_{\max} owing to the lower heat flux entering the domain. As the aspect ratio decreases, the external transfer area increases, thus raising the heat flux input and the efficiency. There is a maximum efficiency that is reached for $\phi_0 = 0.033$ over the whole range [0.4–2]. However, for values \tilde{H}/\tilde{L} less than 0.4, curves with $\phi_0 \leq 0.063$ present an absolute maximum of efficiency, while for curves with $\phi_0 > 0.063$, the efficiency keeps increasing as \tilde{H}/\tilde{L} decreases. The curve with $\phi_0 = 0.043$ is the optimal value sought, which generates the maximum absolute efficiency throughout the range of variation, as can be seen in the extension of that area in Fig. 6b. After successive simulations, with the variable ranges shown in Table 1,

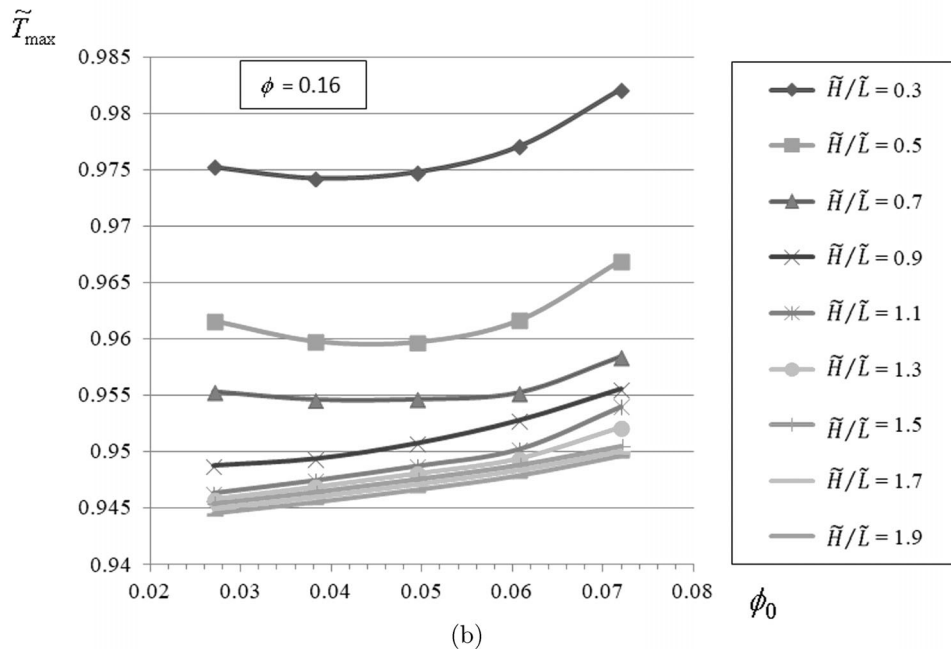
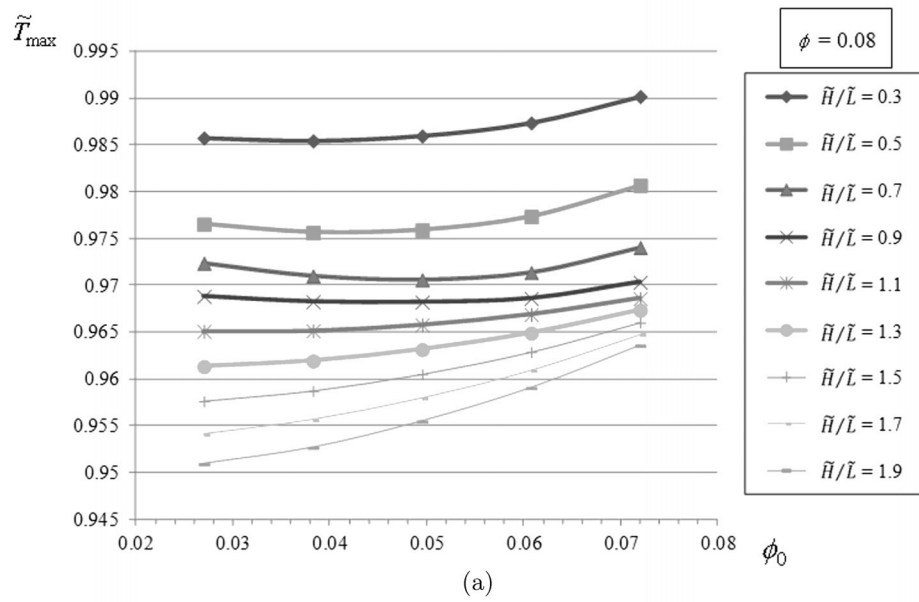


Fig. 9. \tilde{T}_{\max} vs. ϕ_0 for different \tilde{H}/\tilde{L} with (a) $\phi = 0.08$, $\tilde{H}_1/\tilde{L}_1 = 0.4$, $\tilde{H}_0/\tilde{L}_0 = 0.4$, and $\tilde{H}_2 = 0.1$; (b) $\phi = 0.16$, $\tilde{H}_1/\tilde{L}_1 = 0.4$, $\tilde{H}_0/\tilde{L}_0 = 0.4$, and $\tilde{H}_2 = 0.1$.

the maximum absolute efficiency is reached for $\phi_0 = 0.043$, $\tilde{H}/\tilde{L} = 0.3$, $\tilde{H}_0/\tilde{L}_0 = 0.4$, $\tilde{H}_1/\tilde{L}_1 = 0.4$, and $\tilde{H}_2 = 0.1$.

Table 4 summarizes the designs of minimum \tilde{T}_{\max} and maximum ξ for $\phi = 0.1$. Figure 7 presents isotherms over the optimal configurations of Table 4. In Fig. 7, the maximum efficiency configuration shows greater penetration of the high temperature isotherms (red colour) over the blade domain, more heat transferred. On the other hand, the configuration with the minimum maximum temperature maintains the high temperature isotherms near the outer edge, where ellipses 1 transfer most of the heat entering the domain.

Then the behaviour of \tilde{T}_{\max} and the heat evacuation efficiency varying the material ratio ϕ is analysed.

As shown in Fig. 8a, there is a minimum \tilde{T}_{\max} for optimal values of \tilde{H}_2 when ϕ is equal to or less than 0.14, i.e., when the conduit sizes are small enough. The optimal design groups the conduits most closely to each other at the expense of larger distance travelled by the heat flow. This behaviour is not hold for ϕ values over 0.14 (Fig. 8a). On the other hand, the heat evacuation efficiency increases practically linearly as \tilde{H}_2 decreases for all the ϕ range, which reduces the distance travelled by the heat flow and increases the net heat transferred, as seen in Fig. 8b.

The thermal behaviour of the blade with \tilde{H}/\tilde{L} and ϕ_0 for different ϕ values is similar to that already described for $\phi = 0.1$. This fact is exemplified in Figs. 9a and 9b for $\phi = 0.08$ and 0.16, respectively, where relocation of the curves toward lower values \tilde{T}_{\max} is observed, the increase in ϕ conserving practically the same tendency. The same happens with the efficiency for ϕ from 0.08 to 0.16. The curves show a shift toward higher efficiency values, practically maintaining the same shape. Such a situation is illustrated in Figs. 10a and 10b.

6. DISCUSSION

As might be expected, the optimal wall thickness \tilde{H}_2 for the maximum efficiency (or minimum thermal resistance) corresponds to the lowest range value, meaning the smaller path travelled by heat. However, it is remarkable that to get the minimum \tilde{T}_{\max} , the optimal wall thickness \tilde{H}_2 does not correspond to the smaller value, conversely it could be find placed between the extremes range values. To exemplify this, Fig. 11 shows isotherms for two identical geometries, only the wall thickness differing. The figure on the left corresponds to $\tilde{H}_2 = 0.1$ and that on the right, to $\tilde{H}_2 = 0.3$. In both cases, the point of maximum temperature is located in the upper corner over the ellipse 0 side, corresponding to the farthest point from the ellipses. As can be seen, the case on the right shows a greater penetration of higher temperature isotherms, flatter isotherms generated and the heat flux over ellipse 0 decreasing by approximately 3%. In the same way, as ellipse 1 moves away from the outer edge, it generates a decrease by more than 7% in the heat evacuated by ellipse 1, generating a decrease in \tilde{T}_{\max} by 12% (for $T_{\infty} - T_{\min} = 600^{\circ}\text{C}$, it corresponds to a reduction of 72°C). This optimal distribution of the isotherms reduces the heat flux entering the domain by 6%, which is beneficial due to the lower energy extracted to the combustion gases and the lower maximum temperature on the metal.

The Constructal designs for maximum ξ and minimum \tilde{T}_{\max} were achieved with similar conduit sizes ($\phi_0 \approx 0.033$) and different \tilde{H}/\tilde{L} values. However, for the same \tilde{H}/\tilde{L} value, it is possible to generate small differences in the minimum \tilde{T}_{\max} and the maximum ξ by varying only ϕ_0 . To exemplify that, Fig. 12 plots isotherms over two identical geometries, where only the relative conduit size was changed. There, the figure on the left represents conduits of equal sizes, while the figure on the right depicts a configuration where ellipse 0 takes 53% of the total area belonging to the conduits. In the figure on the right, a greater ellipse 0 size led to an increase of 36% in the heat evacuation. The reason can be that the increase in hydraulic diameter led to a raise in the convection coefficient. In turn, the reduction in the ellipse 1 size generates a drop of 20% in its heat transferred. Overall, the figure on the right presents a reduction of 13% in the total heat evacuated, which decreases the maximum temperature by 6%. For example, for $T_{\infty} - T_{\min} = 600^{\circ}\text{C}$, it is a reduction of 36°C in the maximum temperature. This example clearly shows that the most efficient relative conduit size (Fig. 12, left side) never coincides with the one that generates the minimum \tilde{T}_{\max} .

7. CONCLUSIONS

Aimed at increasing the GT efficiency, this work relies on the EGTB cooling model [3], which replaces circular conduits with elliptical conduits with a variable aspect ratio. The optimal design was studied with different fixed material ratios for two different objectives: minimization of the maximum temperature over the metal blade and maximization of the heat evacuation efficiency. Both the objectives were achieved by exhaustive searching using the Constructal Theory. The blade temperature field was calculated with solving the diffusion equation by the finite element method, including the heat transfer by convection and radiation from the boundaries. The external thermal barrier coating was also modelled.

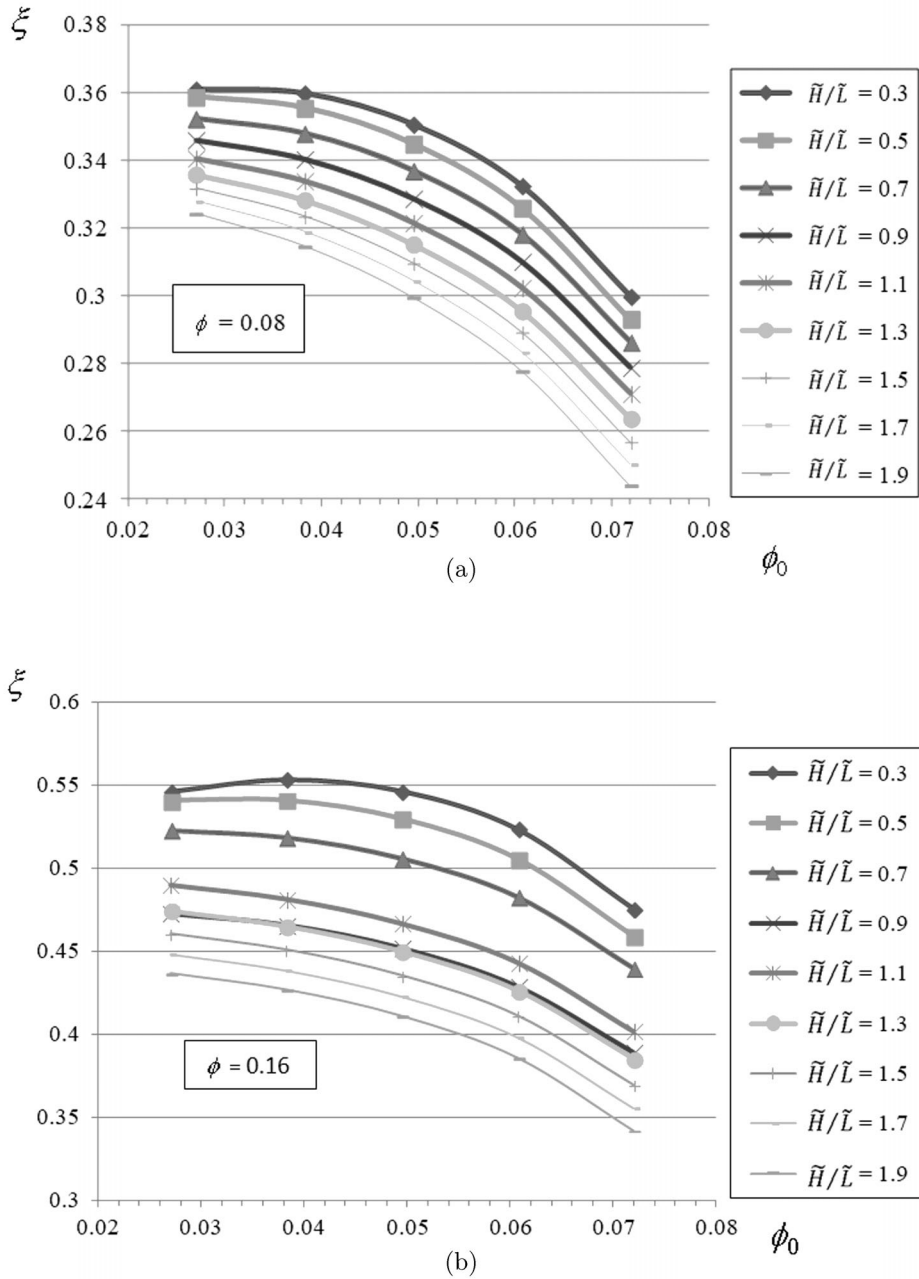


Fig. 10. ξ vs. ϕ_0 for different \tilde{H}/\tilde{L} with (a) $\phi = 0.08$, $\tilde{H}_1/\tilde{L}_1 = 0.4$, $\tilde{H}_0/\tilde{L}_0 = 0.4$, and $\tilde{H}_2 = 0.1$; (b) $\phi = 0.16$, $\tilde{H}_1/\tilde{L}_1 = 0.4$, $\tilde{H}_0/\tilde{L}_0 = 0.4$, and $\tilde{H}_2 = 0.1$.

Using elliptical conduits of aspect ratio 2:5 ($\tilde{H}_0/\tilde{L}_0 = \tilde{H}_1/\tilde{L}_1 = 0.4$) leads to improvement in the thermal performance of cooled blades both in terms of the heat evacuation efficiency and the minimum maximum temperature on the blade. As compared with circular conduits of the same area, elliptical conduits enable transfer of greater amounts of heat and, with a correct design, a lower maximum temperature on the metal. The influence of the conduit aspect ratio on \tilde{T}_{\max} and ξ is considerably lower than the influence of the domain aspect ratio \tilde{H}/\tilde{L} and the relative conduit size ϕ_0 .

The blade designs that generate the minimum maximum relative temperature \tilde{T}_{\max} and maximum heat evacuation efficiency ξ are not identical in terms of the wall thickness \tilde{H}_2 , the domain aspect ratio \tilde{H}/\tilde{L} , or the relative conduit sizes ϕ_0 . The heat evacuation efficiency obtained is the inverse of the thermal

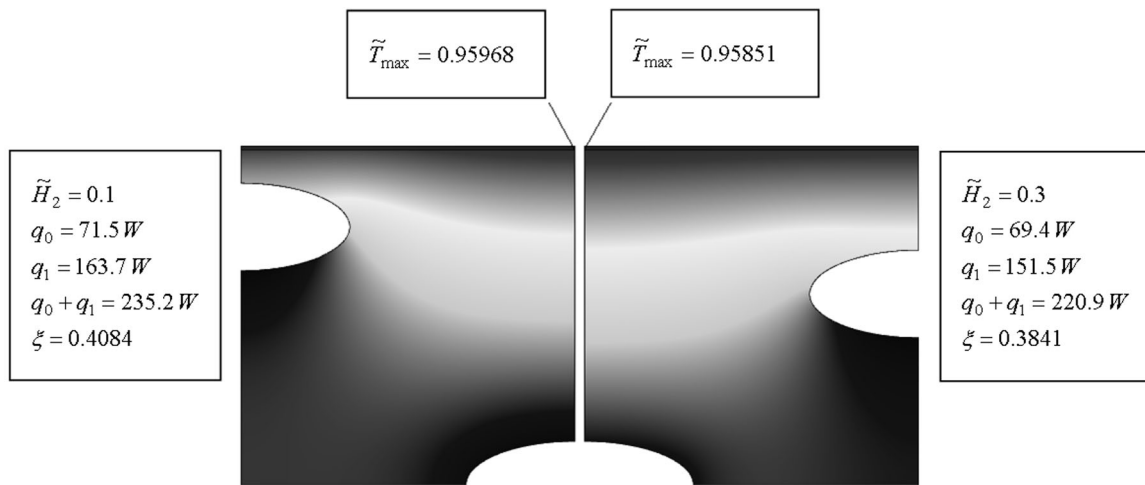


Fig. 11. Thermal behaviour for different wall thickness (different \tilde{H}_2) with $\phi = 0.1$, $\phi_0 = 0.033$, $\tilde{H}/\tilde{L} = 1$, $\tilde{H}_1/\tilde{L}_1 = 0.4$, and $\tilde{H}_0/\tilde{L}_0 = 0.4$.

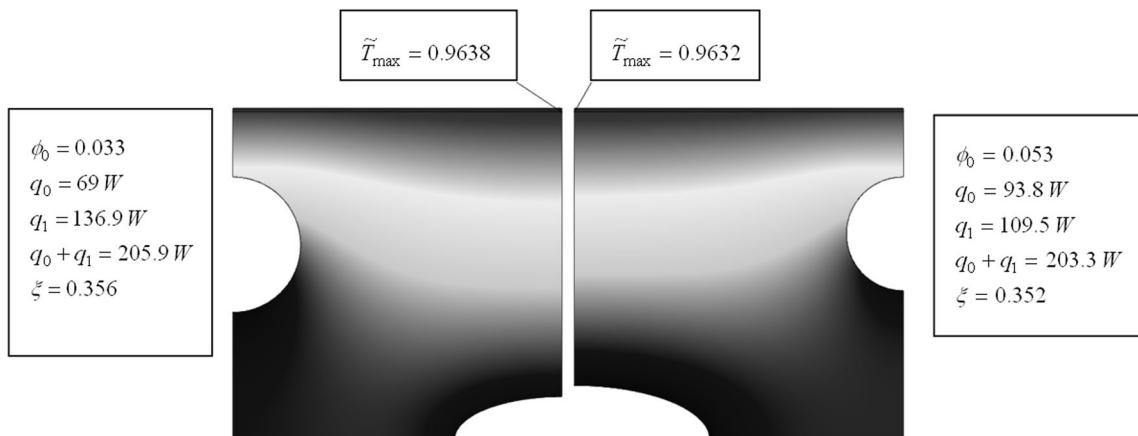


Fig. 12. Thermal behaviour for different relative conduits size (different ϕ_0) with $\phi = 0.1$, $\tilde{H}/\tilde{L} = 1$, $\tilde{H}_0/\tilde{L}_0 = 0.4$, $\tilde{H}_1/\tilde{L}_1 = 1$, and $\tilde{H}_2 = 0.2$.

resistance of the analysed domain defined by Feng et al. [4]. So, it can be inferred that the objectives of minimum maximum temperature \tilde{T}_{\max} or minimum thermal resistance lead to different designs.

The domain aspect ratios \tilde{H}/\tilde{L} for minimization of \tilde{T}_{\max} and maximization of ξ are optimal at the opposite ends of the range, leading to different optimal relative conduit size and wall thickness and thus to a different external blade design, as shown in Table 2 and Fig. 7. For greater efficiency, the temperature profile depicts deeper penetration of high temperature isotherms, while for lower maximum temperature, the distance between two consecutive ellipses 1 (for two consecutive domains) must be minimized, the high temperature isotherms kept near the outer edge of the domain.

In designs with a material ratio of 10% and the same domain aspect ratio, it was possible to obtain different optimal values of relative conduit size and wall thickness, which implies slight variations in the efficiency and maximum temperature on the metal. The reason is that when the conduit design on the domain varies, so does the distribution of temperatures (isotherms), which directly influences the incoming heat. Although the reduction in the maximum temperature or the rise in the heat evacuated could seem insignificant, the relevance of the improvement will depend on the total domain size, which is dimensionless in this work.

NOTATIONS

A —area, dm^2

D_h —hydraulic diameter
 f —Darcy friction coefficient
 H —elemental blade height, dm
 h —convection coefficient, $W/(m^2 \cdot K)$
 H_0 —vertical semi-axis of the ellipse 0, dm
 H_1 —vertical semi-axis of the ellipse 1, dm
 H_2 —wall thickness of ellipse 1, dm
 k —thermal conductivity coefficient, $W/(m \cdot K)$
 L —elemental blade width, dm
 L_0 —horizontal semi-axis of the ellipse 0, dm
 L_1 —horizontal semi-axis of ellipse 1, dm
 Nu —Nusselt number
 ε —emissivity
 μ —dynamic viscosity, $kg/m \cdot s$
 ν —cinematic viscosity, m^2/s
 ξ —heat evacuation efficiency
 ρ —density, kg/m^3
 P —pressure
 Pe —Peclet number
 Pr —Prandtl number
 q —total heat, W
 R —thermal resistance, $m^2 \cdot K/W$
 Re —Reynolds number
 S —heat source, W/m^3
 T —temperature, K
 V —velocity, m/s
 W —transversal dimension, dm
 x —abscissa coordinate, dm
 y —ordinates coordinate, dm
 σ —Stefan–Boltzmann constant, $W/(K^4 m^2)$
 ϕ —material ratio
 ϕ_0 —1/4 ellipse 0 dimensionless area
 ϕ_1 —1/2 ellipse 1 dimensionless area

Superscript

\sim —non dimensional parameter

Subscripts

0—ellipse 0
 1—ellipse 1
 max—maximum
 min—minimum

REFERENCES

1. Han, J.C., Dutta, S., and Ekkad, S., *Gas Turbine Heat Transfer and Cooling Technology*, New York: Taylor and Francis, 2012.
2. Bejan, A. and Lorente, S., *Design with Constructal Theory*, Wiley, 2008.
3. Rocha, L.A., Bejan, A., and Lorente, S., *Constructal Law and the Unifying Principle of Design*, New York: Springer-Verlag, 2013.
4. Feng, H., Chen, L., Xie, Z., and Sun, F., Constructal Design for Gas-Turbine Blade Based on Minimization of Maximum Thermal Resistance, *Appl. Therm. Engin.*, 2015, vol. 90, pp. 792–797.
5. Hylton, L.D., Mihelc, M.S., Turner, E.R., Nealy, D.A., and York, R.E., *Analytical and Experimental Evaluation of the Heat Transfer Distribution Over the Surfaces of Turbine Vanes*, NASA, 1983.
6. Reyhani, M.R., Rezazadeh, M., Alizadeh, M., Fathi, A., and Khaledi, H., Turbine Blade Temperature Calculation and Life Estimation, a Sensitivity Analysis, *Propul. Power Res.*, 2013, pp. 148–171.
7. David R.C., Matthias, O., and Nitin, P.P., Thermal-Barrier Coatings for More Efficient Gas-Turbine Engines, *Mat. Res. Soc. Bull.*, 2012, vol. 37, no. 10, pp. 891–898.
8. Han, J.C., Recent Studies in Turbine Blade Cooling, *Int. J. Rotat. Machin.*, 2004, vol. 10, no. 6, pp. 443–457.
9. Han, J.C. and Wright, L.M., Enhanced Internal Cooling of Turbine Blades and Vanes, Turbine Heat Transfer Laboratory, Department of Mechanical Engineering, University College Station Texas, USA, 2013.
10. Bunker, R.S., Cooling Design Analysis, GE Global Research, One Research Circle and US DOE, New York, 2006.
11. Sundberg, J., Heat Transfer Correlations for Gas Turbine Cooling; <http://www.diva-portal.org/smash/get/diva2:21321/FULLTEXT01.pdf>//site visited 06/06/16.
12. Al-Luhaibi, A.J., and Tariq, M., Thermal Analysis of Cooling Effect on Gas Turbine Blade, *Int. J. Res. Engin. Tech.*, 2014, pp. 603–610.
13. Iacovides, H. and Raisee, M., Flow and Heat Transfer in Straight Cooling Passages with Inclined Ribs on Opposite Walls: An Experimental and Computational Study, *Exp. Therm. Fluid Sci.*, 2003, pp. 283–294.
14. Ravi Teja, T. and Krishna Chaitanya, S., Case Study on Turbine Blade Internal Cooling, *Int. J. Engin. Res. Tech. (IJERT)*, 2013, vol. 2, no. 3, pp. 1–5.
15. Nasir, H., Turbine Blade Tip Cooling and Heat Transfer, Doctoral Dissertation, Bangladesh University of Engineering and Technology, 2004.
16. Han, J.C. and Srinath, E., Recent Development in Turbine Blade Film Cooling, *Int. J. Rotat. Machin.*, 2001, vol. 7, no. 1, pp. 21–40.
17. Xu, R., Hou, J., Wang, L., Yu, Y., Wei, J., and Li, C., Fluid Flow and Heat Transfer Characteristics in a 180-Deg Round Turned Channel with a Perforated Divider, *J. Appl. Math. Phys.*, 2014, pp. 411–417.
18. Yuri, M., Masada, J., Tsukagoshi, K., Ito, E., and Hada, S., Development of 1600°C-Class High-Efficiency Gas Turbine for Power Generation Applying J-Type Technology, *Mitsubishi Heavy Ind. Techn. Rev.*, 2013, vol. 50, no. 3, pp. 1–10.
19. Ahn, J., Schobeiri, M.T., Han, J.-C., and Moon, H.-K., Effect of Rotation on Leading Edge Region Film Cooling of a Gas Turbine Blade with Three Rows of Film Cooling Holes, *Int. J. Heat Mass Transfer*, 2007, vol. 50, no. 12, pp. 15–25.
20. Siddique, W., Design of Internal Cooling Passages: Investigation of Thermal Performance of Serpentine Passages, Doctoral Dissertation, Stockholm: Royal Institute of Technology, 2011.
21. Ferlauto, M., An Inverse Method of Designing the Cooling Passages of Turbine Blades Based on the Heat Adjoint Equation, *Proc. Inst. Mech. Engin., Part A: J. Power Energy*, 2014, vol. 228, no. 3, pp. 328–339.
22. Alhajeri, M.H., Alhamad Alhajeri, H., Alrajhi, J., Alardhi, M., and Alshaye, S., Numerical Analysis of Fluid Flow in Turbine Blade Cooling Passage, *Int. J. Sci. Adv. Tech.*, 2011, vol. 1, no. 8, pp. 1–10.
23. Schlichting, H., *Boundary-Layer Theory*, 6th ed., New York: McGraw-Hill, 1979.
24. Cengel, Y.A., *Heat and Mass Transfer*, 3rd ed., McGrawHill, 2007.